

## GRAPHENE AS A TEMPLATE AND STRUCTURAL SCAFFOLD FOR THE SYNTHESIS OF 3D POROUS BIO-ADSORBENT

ZHUANG Y.<sup>1</sup>, YU F.<sup>3</sup>, MA J.<sup>1</sup> and CHEN J.<sup>1,2</sup>

<sup>1</sup> State Key Laboratory of Pollution Control and Resource Reuse, School of Environmental Science and Engineering, Tongji University, 1239 Siping Road, Shanghai 200092, P. R. of China, <sup>2</sup> Department of Mechanical Engineering, University of Wisconsin–Milwaukee, Milwaukee, WI 53211, USA, <sup>3</sup> College of chemistry and environmental engineering, Shanghai Institute of Technology, Shanghai 2001418, China  
E-mail: jma@tongji.edu.cn, jhchen@tongji.edu.cn

### ABSTRACT

Graphene-soy protein (GS) aerogel was prepared by a simple thermal reduction method and then used as an adsorbent for the removal of antibiotics. The GS aerogel were characterized by optical contact angle meter, scanning electron microscopy (SEM), transmission electron microscopy (TEM), X-ray diffraction (XRD), Raman, Branauer-Emmett-Teller (BET) and Fourier transform infrared spectroscopy (FTIR). In GS, graphene acts as a template that loads onto the surface of protein through hydrogen bonds to form a layered bulk unit and interacts with each other to form self-assembled hydrogels. Moreover, graphene interacts well with protein without obvious structural damage and does not agglomerate. In Raman, there is a slight increase of the intensity ratio of the D peak to G peak (ID/IG) for the GS compared with GN which demonstrated the successful incorporation of graphene into protein without obvious structural damage. The resulting GS has a high specific area of 30.07 m<sup>2</sup>/g with abundant microspores and excellent hydrophilic properties. The macropore, mesopore, and micropore of GS are 0.009, 0.714, and 0.120 cm<sup>3</sup>/g, respectively. The average pore size of GS is 10.23 nm. GS has excellent adsorption properties for tetracycline (500.0 mg/g) and ciprofloxacin (500.0 mg/g). This result suggests that the small quantity of graphene assisted the protein to form an excellent bio-adsorbent.

**Keywords:** graphene, protein, adsorption, antibiotics

### 1. Introduction

In the past several years, free-standing two-dimensional monolayer graphene with excellent properties has caught global attention and has been adopted for various applications (Yu, Bo et al. 2011, Wen, Cui et al. 2012, Vadahanambi, Lee et al. 2013). Graphene has been considered as an excellent adsorbent in environmental applications due to their high SSA (2630 m<sup>2</sup>/g). With its delocalized  $\pi$  bonds, graphene can potentially adsorb organic contaminants, especially those with molecules containing  $\pi$ -electrons that can interact with the polarized graphene surface via  $\pi$ - $\pi$  electron coupling or van der Waals interactions (Lin, Xu et al. 2013, Chen, Gao et al. 2014). Compared with polymers, graphene composites may have better hydrophilicity, biological compatibility, and lower cytotoxicity; moreover, gels can be prepared at a large scale by a facile gelation process in a short period of time. However, graphene nanosheets tend to aggregate due to interplanar interactions (Chowdhury and Balasubramanian 2014). In addition, most forms of graphene materials are not well dispersible or soluble in most common solvents due to their low hydrophilicity, poor biocompatibility and few functional groups, and high cost. These above factors limit their applications as adsorbents. The use of biocompatible hydrophilic biopolymers may improve water solubility properties of nanomaterials.

Therefore, it is reasonable to predict that the biopolymer-mediated graphene gels may function as porous adsorbents with satisfactory adsorption capacity and limited toxicity for applications in wastewater treatment (Cheng, Deng et al. 2013). As an adsorbent, three-dimensional (3D)

graphene adsorbents can be easily separated in the aqueous solution. Developing hydrophilic and biocompatible 3D bio-adsorbents with a large SSA and unique mesoporosity will expand their significance in environmental applications (Zhao, Wang et al. 2014). Cheng *et al.* (Cheng, Deng et al. 2013) prepared three typical graphene oxide (GO)-biopolymer gels (bovine serum albumin, chitosan, and double-stranded DNA) for the first time and investigated the adsorption capabilities of dyes and heavy metals. The GO-biopolymer gels displayed an adsorption capacity as high as 1100 mg/g for methylene blue dye and 1350 mg/g for methyl violet dye, respectively. Thus, it can be seen that graphene and polymers can form gels to be used as bio-adsorbents; however, the combination ways of graphene with polymers and the characteristics of the resulting materials still need further study.

In this paper, a graphene assisted 3D porous soy protein aerogel (GS) is prepared by a simple thermal reduction method, and then the GS is used as an adsorbent for the removal of antibiotics from aqueous solutions. This method is inexpensive, simple, and features a high-yield. In the synthesis process of GS, graphene acts as a template that is loaded onto the surface of the protein to form a layered bulk unit. More importantly, graphene also acts as a structural scaffold to form 3D hydrogels through self-assembly, which can be turned into porous aerogels after freeze drying. The protein combines well with graphene in the GS, and the resulting GS possesses high hydrophilicity and excellent adsorption properties for antibiotics.

## **2. Experimental**

### **2.1. Materials**

All chemicals were purchased from Sinopharm Chemical Reagent Co., Ltd. (Shanghai, China) in analytical purity and were used in the experiments without any further purification. All solutions were prepared using deionized water.

### **2.2. Preparation of graphene-soy protein aerogels**

Graphite oxide was obtained using the modified Hummers' method (Hummers and Offeman 1958, Hirata, Gotou et al. 2004, Mao, Pu et al. 2012), dispersed in deionized water, and sonicated in an ultrasound bath for 12 h. Soy protein and ascorbic acid were added to the GO dispersion and placed into an ultrasound bath for 5 h to form a uniform solution. The mass ratio of graphene to soy protein was 1:6; the resulting products were denoted as GS. The mixture was heated in a water bath under 90°C for 12 h to form hydrogels. The aerogels were synthesized after the hydrogels were washed with distilled water for several times and then freeze-dried for 24 h. For comparison, graphene aerogel (GN) without protein was also prepared as described above.

### **2.3. Characterization methods**

The surface morphologies of GN and GS were visualized using a field-emission SEM (Hitachi, S-4800), AFM (NanoScope III a MultiMode) and TEM (JEOL, JEM-2010). The hydrophilicities were characterized by an optical contact angle meter (Dataphysics, OCA-20). Measurements of micro-Raman spectra were carried out using a Raman Scope system (LabRam, 1B) with a 532 nm wavelength incident laser light and 20 mW power. XRD were collected on a Bragg-Brentano diffractometer (Rigaku, D/Max-2200) with monochromatic Cu K $\alpha$  radiation ( $\lambda = 1.5418 \text{ \AA}$ ) of a graphite curve monochromator, and the data were collected from  $2\theta = 2\text{-}40^\circ$  at a continuous scan rate of  $2^\circ/\text{min}$  for phase identification. The BET isotherms were measured by an Accelerated Surface Area and Porosimetry system (Micromeritics, ASAP 2020). A UV-visible absorption-based approach is used for a direct evaluation of the protein content released from GS (Attal, Thiruvengadathan et al. 2006, Jeong, Kim et al. 2007). A calibration plot is then made by monitoring the intensity of the peak as a function of the true concentration of the CNTs. Earlier reference stated that the adsorption peak at 280 nm is a signature of the soy protein.

### **2.4. Batch sorption experiments**

Batch experiments were conducted to evaluate the adsorption performance of antibiotics on the adsorbents. GN and GS were selected as adsorbents for antibiotics adsorption in an aqueous solution. The residual concentrations in the solution were determined by an ultraviolet spectrophotometer (Tianmei UV-2310(II)) at 360 nm for tetracycline and 270 nm for

ciprofloxacin. The adsorption isotherm was studied at pH=6, and the initial concentration was set from 1 mg/L to 50 mg/L. The adsorption capacity (mg/g) was calculated using Equation (1)

$$q_t = (C_0 - C_t) \times \frac{V}{m} \quad (1)$$

where  $C_0$  and  $C_t$  are the initial concentration and the concentration after a period of time  $t$  (mg/L);  $V$  is the initial solution volume (L); and  $m$  is the adsorbent dosage (g).

Adsorption isotherms were fitted using Langmuir and Freundlich models, which were used to evaluate the adsorption equilibrium, as shown in Equations (2) and (3). Another important parameter,  $R_L$ , called the separation factor or equilibrium parameter, can be used to determine the feasibility of adsorption in a given concentration range over adsorbent, as shown by Equation (4) (Li, Liu et al. 2013).

$$\frac{C_e}{q_e} = \frac{1}{K_L} + \left(\frac{\alpha_L}{K_L}\right)C_e \quad (2)$$

$$\ln q_e = \ln K_F + \frac{1}{n} \ln C_e \quad (3)$$

$$R_L = \frac{1}{1 + K_L C_0} \quad (4)$$

where  $K_L$  (L/g) and  $\alpha_L$  (L/mg) are the Langmuir isotherm constants, and  $\alpha_L$  relates to the energy of adsorption. When  $C_e/q_e$  is plotted against  $C_e$ , a straight line will be obtained. The value of  $K_L$  can be obtained from the intercept, which is  $1/K_L$ , and the value of  $\alpha_L$  can be obtained from the slope, which is  $\alpha_L/K_L$ . The maximum adsorption capacity of the adsorbent,  $q_{m,cal}$ , i.e., the equilibrium monolayer capacity or saturation capacity, is numerically equal to  $K_L/\alpha_L$ ;  $K_F$  is the adsorption constant of the Freundlich model, and  $n$  is the Freundlich linearity index. The Langmuir model is ideal, as it possesses a perfect adsorbent surface and monolayer molecule adsorption. As an empirical model, the Freundlich model is used widely in the field of chemistry.

### 3. Results and discussion

#### 3.1. Morphological and microstructure of GN and GS

Digital images of graphite oxide, protein, GS, and GN hydrogels are shown in Fig.1 (a). It can be observed that both GN and GS hydrogels have uniform structures; however, the GN hydrogel is much looser than the GS hydrogel, and the GN hydrogel floats while the GS hydrogel remains at the bottom.

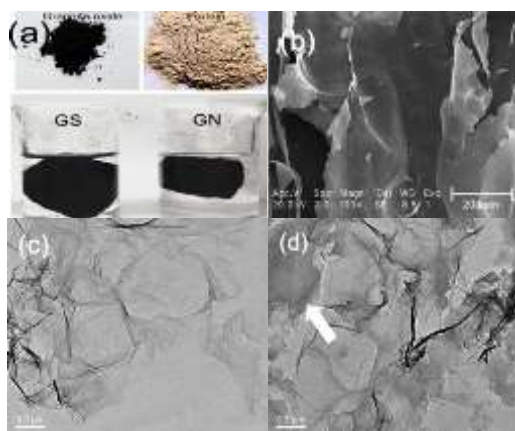
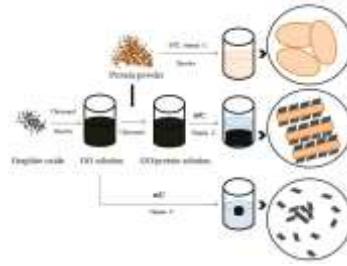


**Figure1:** Morphology and microstructure of GN and GS: (a) photographs of GN and GS hydrogels, (b) SEM of GS, (c) TEM of GN, and (d) TEM of GS.



**Schematic 1:** Preparation process of GS.

To verify the combination of graphene and protein, we investigated the microstructure of GN and GS aerogels. An SEM of GS is shown in Fig. 1b, and it can be easily seen that GS has a rough structure with layers, indicating pore interactions between nanofillers and the matrix (Rodríguez-González, Martínez-Hernández et al. 2012, Huang, Li et al. 2013). As a result, the proteins are separated into layers of graphene. From Fig. 1d, it can be seen that in GS the protein (as pointed by the arrow in Fig. 1d) exists on the edge of graphene, and in GS the graphene around the protein appears to be much closer together than in GN as shown in Fig. 1c.

### 3.2. Composition and structure analysis

XRD spectra of GN and GS are presented in Fig. 2a, and Raman spectra of GN and GS are presented in Fig. 2b. In Fig. 2a, no peak appears at  $2\theta$  of 10.6 degree, proving that graphene oxide is partially reduced during the hydrogel preparation for both GN and GS. In Fig. 3c,  $2\theta$  of around 25 degree of GN is the characteristic peak of freeze-dried graphene aerogel (Xu, Sheng et al. 2010), which further proves that the nanosheet in this biocomposite is graphene rather than graphene oxide. Moreover, the characteristic peak in GS is to the left of that of GN. Since the lattice parameters of GS are larger than GN, this further proves that the protein prevented the graphene from agglomeration. In Fig. 2b, the slight increase of the intensity ratio of the D peak to G peak ( $I_D/I_G$ ) for the GS compared with GN demonstrated the successful incorporation of graphene into protein without obvious structural damage (Gao, Liu et al. 2014). Fig. 2c shows the  $N_2$  adsorption-desorption isotherms of GS and protein. The isotherms of GN exhibit a typical type-I curve and a hysteresis loop at a relative pressure of 0.4, indicating the presence of slit-shaped pores between parallel layers of graphene (Ferrari 2007). The specific areas of GS and GN are  $30.07 \text{ m}^2/\text{g}$  and  $119.17 \text{ m}^2/\text{g}$  respectively, while the protein specific area is about  $0 \text{ m}^2/\text{g}$ . The pore size distribution of GS is also shown in Fig. 2d. The macropore, mesopore, and micropore of GS are  $0.009$ ,  $0.714$ , and  $0.120 \text{ cm}^3/\text{g}$ , respectively. The average pore size of GS is  $10.23 \text{ nm}$ .

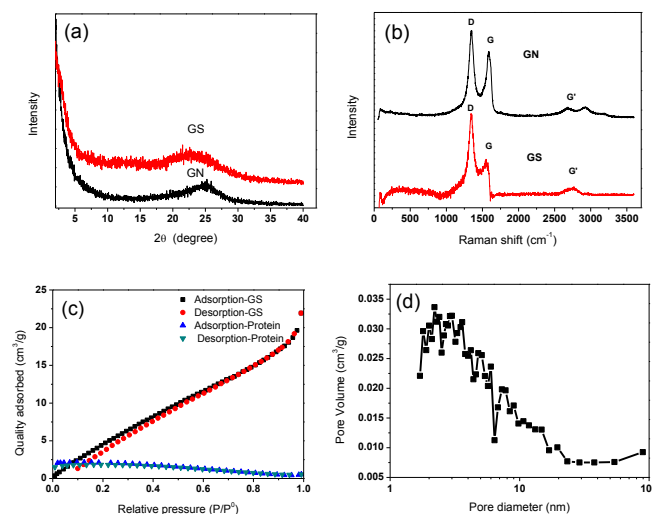


**Figure 2:** Composition and structure analysis (a) XRD of GN and GS, (b) Raman of GN and GS, (c)  $N_2$  adsorption and desorption curves of GS and protein, (d) pore size distribution of GS.

### 3.3. Antibiotics adsorption

The adsorption isotherms were calculated by Langmuir and Freundlich models, as shown in Fig. 3a and 3b, respectively. Based on the  $R^2$  values, it can be seen from Table 1 that the adsorption isotherms fit well by both the Langmuir and the Freundlich models. It could be calculated from the Langmuir isotherm equation that the maximum theoretical adsorption capacities of the two antibiotics on GS were both 500.0 mg/g.

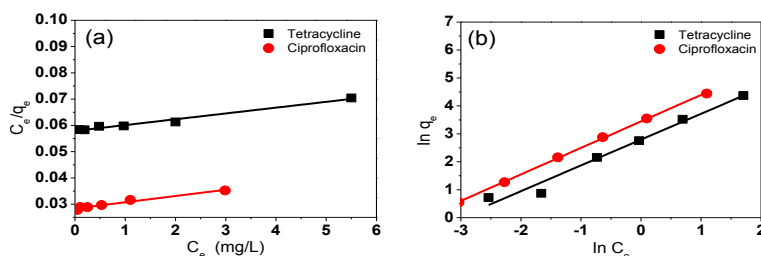


**Figure 3:** Antibiotics adsorption properties, antibiotics adsorption capacities (a) of protein, GS and GN, adsorption isotherm (b), Langmuir isotherm (c) and Freundlich isotherms (d) of antibiotics on GS.

### 4. Conclusions

A graphene-assisted 3D porous soy protein aerogel (GS) is prepared by a simple method and then used as an adsorbent for the removal of antibiotics. The GS aerogel has good hydrophilicity and abundant functional groups. Moreover, unlike protein which does not contain any nano-pores, the GS has a large specific surface area. The graphene in GS turned out to be separated by protein and was prevented from aggregation. The resulting GS possesses excellent adsorption properties. As protein is inexpensive and nontoxic, the porous biocomposite aerogel has significant potential for use as an adsorbent for biological applications.

### REFERENCES

1. Attal, S., R. Thiruvengadathan and O. Regev (2006). "Determination of the concentration of single-walled carbon nanotubes in aqueous dispersions using UV-visible absorption spectroscopy." *Analytical Chemistry* **78**(23): 8098-8104.
2. Chen, H., B. Gao and H. Li (2014). "Functionalization, pH, and ionic strength influenced sorption of sulfamethoxazole on graphene." *J. Environ. Chem. Eng.* **2**(1): 310-315.
3. Cheng, C. S., J. Deng, B. Lei, A. He, X. Zhang, L. Ma, S. Li and C. Zhao (2013). "Toward 3D graphene oxide gels based adsorbents for high-efficient water treatment via the promotion of biopolymers." *Journal of Hazardous Materials* **263 Pt 2**: 467-478.
4. Chowdhury, S. and R. Balasubramanian (2014). "Recent advances in the use of graphene-family nanoadsorbents for removal of toxic pollutants from wastewater." *Adv Colloid Interface Sci* **204**: 35-56.
5. Ferrari, A. C. (2007). "Raman spectroscopy of graphene and graphite: Disorder, electron-phonon coupling, doping and nonadiabatic effects." *Solid State Communications* **143**(1-2): 47-57.
6. Gao, C., T. Liu, C. Shuai and S. Peng (2014). "Enhancement mechanisms of graphene in nano-58S bioactive glass scaffold: mechanical and biological performance." *Sci Rep* **4**: 4712.
7. Hirata, M., T. Gotou, S. Horiuchi, M. Fujiwara and M. Ohba (2004). "Thin-film particles of graphite oxide 1." *Carbon* **42**(14): 2929-2937.
8. Huang, L., C. Li, W. Yuan and G. Shi (2013). "Strong composite films with layered structures prepared by casting silk fibroin-graphene oxide hydrogels." *Nanoscale* **5**(9): 3780-3786.
9. Hummers, W. S. and R. E. Offeman (1958). "Preparation of graphitic oxide." *J. Am. Chem. Soc.* **80**(3): 1339-1340.
10. Jeong, S. H., K. K. Kim, S. J. Jeong, K. H. An, S. H. Lee and Y. H. Lee (2007). "Optical absorption spectroscopy for determining carbon nanotube concentration in solution." *Synthetic Metals* **157**(13-15): 570-574.
11. Li, R., L. Liu and F. Yang (2013). "Preparation of polyaniline/reduced graphene oxide nanocomposite and its application in adsorption of aqueous Hg(II)." *Chemical Engineering Journal* **229**: 460-468

12. Lin, Y., S. Xu and J. Li (2013). "Fast and highly efficient tetracyclines removal from environmental waters by graphene oxide functionalized magnetic particles." *Chemical Engineering Journal* **225**: 679-685.
13. Mao, S., H. H. Pu and J. H. Chen (2012). "Graphene Oxide and Its Reduction: Modeling and Experimental Progress." *RSC Advances* **7**(2): 2643-2662.
14. Rodríguez-González, C., A. L. Martínez-Hernández, V. M. Castaño, O. V. Kharissova, R. S. Ruoff and C. Velasco-Santos (2012). "Polysaccharide Nanocomposites Reinforced with Graphene Oxide and Keratin-Grafted Graphene Oxide." *Ind. Eng. Chem. Res.* **51**(9): 3619-3629.
15. Vadahanambi, S., S. H. Lee, W. J. Kim and I. K. Oh (2013). "Arsenic removal from contaminated water using three-dimensional graphene-carbon nanotube-iron oxide nanostructures." *Environmental Science & Technology* **47**(18): 10510-10517.
16. Wen, Z. H., S. M. Cui, H. J. Kim, S. Mao, K. H. Yu, G. H. Lu, H. H. Pu, O. Mao and J. H. Chen (2012). "Binding Sn-Based Nanoparticles on Graphene as Anode of Lithium Ions Batteries." *Journal of Materials Chemistry* **22**(8): 3300-3306.
17. Xu, Y., K. Sheng, C. Li and G. Shi (2010). "Self-assembled graphene hydrogel via a one-step hydrothermal process." *ACS Nano* **7**(4): 4324-4330.
18. Yu, K., Z. Bo, G. Lu, S. Mao, S. Cui, Y. Zhu, X. Chen, R. S. Ruoff and J. Chen (2011). "Growth of Carbon Nanowalls at Atmospheric Pressure for One-step Gas Sensor Fabrication." *Nanoscale Research Letters* **6**: 202.
19. Zhao, Z., X. Wang, J. Qiu, J. Lin, D. Xu, C. a. Zhang, M. Lv and X. Yang (2014). "Three-dimensional graphene-based hydrogel/aerogel materials." *Rev. Adv. Mater. Sci.* **36**(2): 137-151.